

(La_{1-x}Ba_x)(Zn_{1-x}Mn_x)AsO: A Two Dimensional “1111” Diluted Magnetic Semiconductor in Bulk Form

Cui Ding¹, Huiyuan Man¹, Chuan Qin¹, Jicai Lu¹, Yunlei Sun¹, Quan Wang¹, Biqiong Yu¹, Chunmu Feng¹, T. Goko², C.J. Arguello², L. Liu², B.J. Frandsen², Y.J. Uemura², Hangdong Wang³, H. Luetkens⁴, E. Morenzoni⁴, W. Han⁵, C. Q. Jin⁵, T. Munsie⁶, T.J. Williams⁶, R.M. D’Ortenzio⁶, T. Medina⁶, G.M. Luke^{6,7}, T. Imai^{6,7}, F.L. Ning^{1,*}

¹*Department of Physics, Zhejiang University, Hangzhou 310027, China*

²*Department of Physics, Columbia University, New York, New York 10027, USA*

³*Department of Physics, Hangzhou Normal University, Hangzhou 310016, China*

⁴*Paul Scherrer Institute, Laboratory for Muon Spin Spectroscopy, CH-5232 Villigen PSI, Switzerland*

⁵*Beijing National Laboratory for Condensed Matter Physics,*

and Institute for Physics, Chinese Academy of Sciences, Beijing 100190, China

⁶*Department of Physics and Astronomy, McMaster University, Hamilton, Ontario L8S4M1, Canada and*

⁷*Canadian Institute for Advanced Research, Toronto, Ontario M5G1Z8, Canada*

(Dated: April 9, 2022)

We report the synthesis and characterization of a bulk diluted magnetic semiconductor (La_{1-x}Ba_x)(Zn_{1-x}Mn_x)AsO ($0 \leq x \leq 0.2$) with a layered crystal structure identical to that of the “1111” FeAs superconductors. No ferromagnetic order occurs for (Zn,Mn) substitution in the parent compound LaZnAsO without charge doping. Together with carrier doping via (La,Ba) substitution, a small amount of Mn substituting for Zn results in ferromagnetic order with T_C up to ~ 40 K, although the system remains semiconducting. Muon spin relaxation measurements confirm the development of ferromagnetic order in the entire volume, with the relationship between the internal field and T_C consistent with the trend found in (Ga,Mn)As, the “111” Li(Zn,Mn)As, and the “122” (Ba,K)(Zn,Mn)₂As₂ systems.

PACS numbers: 75.50.Pp, 71.55.Ht, 76.75.+i

The successful fabrication of III-V ferromagnetic semiconductors (Ga,Mn)As [1] in thin-film form via molecular beam epitaxy (MBE) has triggered extensive research into diluted magnetic semiconductors (DMS) [2–4]. The highest Curie temperatures, T_C , has been reported as ~ 190 K with Mn doping levels at $\sim 12\%$ in (Ga,Mn)As [5]. However, the quality of some thin films is strongly dependent on the preparation procedure and heat treatment, and thus not always controllable [6, 7]. Nonetheless, if properly prepared, (Ga,Mn)As thin films exhibit spatially homogenous ferromagnetism throughout the entire sample volume for a wide range of Mn concentrations, as confirmed by muon spin relaxation (μ SR) measurements [8]. In contrast to the successful use of MBE, the preparation of bulk (Ga,Mn)As has been much more challenging, since the valence mismatch of Mn²⁺ atoms and Ga³⁺ atoms results in severely limited chemical solubility, i.e., $< 1\%$. A similar dilemma was encountered in diluted magnetic oxides (DMO) such as Co-doped ZnO and TiO₂, where ferromagnetism has been observed in thin films but not in bulk materials. The origin of ferromagnetism [7] in these DMO systems is yet to be established.

Seeking for bulk DMS or DMO materials and the investigation of their physical properties may shed light on the origin of ferromagnetism in their thin film counterparts. Furthermore, the availability of bulk specimens would en-

able the use of conventional magnetic probes such as nuclear magnetic resonance (NMR) and neutron scattering, to provide complementary information at a microscopic level. The synthesis of bulk DMS or DMO specimens therefore becomes necessary. Accordingly, Deng et al. [9] followed a theoretical proposal by Masek et al. [10] and doped Mn into the direct-gap semiconductor LiZnAs, thereby successfully synthesizing a bulk I-II-V DMS system, Li(Zn,Mn)As, with ferromagnetic T_C up to 50 K [9] and a cubic crystal structure not identical but very similar to that of the “111” LiFeAs [11] and NaFeAs [12] superconductors. Li(Zn,Mn)As exhibits a very small coercive field of 50 Oe, similar to that of (Ga,Mn)As.

Additionally, Deng et al. [9] demonstrated that hole carriers mediate ferromagnetism in both Li(Zn,Mn)As and (Ga,Mn)As with exchange interactions of comparable magnitude. The growth of Li(Zn,Mn)As compounds, however, suffers from difficulties in the precise control of Li concentrations, making it difficult to understand the interplay between charge carriers and spins [9]. Recently, Zhao et al. [13] reported another ferromagnetic DMS system, (Ba,K)(Zn,Mn)₂As₂, with T_C up to ~ 200 K and a crystal structure identical to that of the “122” (Ba,K)Fe₂As₂ superconductors [14]. In this letter, we report the successful fabrication of a new bulk DMS material, (La_{1-x}Ba_x)(Zn_{1-x}Mn_x)AsO, with T_C up to 40 K and a crystal structure identical to that of the “1111” FeAs superconductor LaFeAsO [15]. This constitutes the third example of a bulk DMS system structurally related to a family of FeAs superconductors.

Chemically stable Ba and Mn atoms are doped into

*Electronic address: ningfl@zju.edu.cn

the parent direct-gap (~ 1.5 eV) semiconductor LaZnAsO [16] to introduce charge carriers and spins, respectively. The system remains paramagnetic for Mn concentrations up to 10% in the absence of Ba doping, but with doped charge carriers to mediate magnetic exchange, static ferromagnetic order develops in $(\text{La}_{1-x}\text{Ba}_x)(\text{Zn}_{1-x}\text{Mn}_x)\text{AsO}$ below $T_C \sim 40$ K as confirmed microscopically by μSR . Semiconducting behavior exists for concentrations up to $x = 0.20$, and pronounced magnetic hysteresis with a coercive field of ~ 1 T has also been observed. Despite the striking difference between the two-dimensional (2D) character of $(\text{La}_{1-x}\text{Ba}_x)(\text{Zn}_{1-x}\text{Mn}_x)\text{AsO}$ and the three-dimensional (3D) structure of $\text{Li}(\text{Zn},\text{Mn})\text{As}$ and $(\text{Ga},\text{Mn})\text{As}$, all three systems exhibit exchange interactions and ordered moments of similar magnitude.

Polycrystalline specimens of $(\text{La}_{1-x}\text{Ba}_x)(\text{Zn}_{1-x}\text{Mn}_x)\text{AsO}$ were synthesized through the solid state reaction method. High purity elements of La, Zn, and As were mixed and heated to 900°C in an evacuated silica tube to produce intermediate products LaAs and ZnAs, which were mixed with ZnO, BaO₂, and Mn with nominal concentrations and slowly heated up to 1150°C , where the mixture was held for 40 hours before cooling at 10°C/h to room temperature. The polycrystals were characterized via X-ray diffraction and dc -magnetization with a Quantum Design SQUID. The electrical resistance was measured on sintered pellets with the typical four-probe method. μSR measurements were performed at Paul Scherrer Institute and TRIUMF.

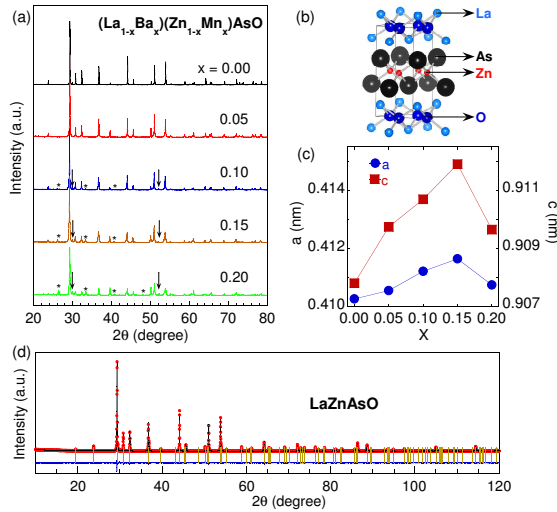


FIG. 1: (Color online). (a) X-ray diffraction pattern of $(\text{La}_{1-x}\text{Ba}_x)(\text{Zn}_{1-x}\text{Mn}_x)\text{AsO}$. Traces of impurity La_2O_3 (\downarrow) and ZnAs_2 ($*$) are marked for $x \geq 0.1$. (b) Crystal Structures of LaZnAsO (P4/nmm). (c) Lattice constants for the a -axis (blue filled circle) and c -axis (red filled square) of $(\text{La}_{1-x}\text{Ba}_x)(\text{Zn}_{1-x}\text{Mn}_x)\text{AsO}$. (d) X-ray diffraction pattern of LaZnAsO with Rietveld analyses.

The crystal structure and X-ray diffraction patterns

are shown in Fig. 1. Bragg peaks from the parent compound LaZnAsO can be well indexed by a ZrCuSiAs-type tetragonal crystal structure (space group P4/nmm), indicating that LaZnAsO is isostructural to LaFeAsO, the parent compound of the “1111” family of Fe-based high temperature superconductors [15]. The Zn atoms, each one tetrahedrally coordinated to four As atoms, form parallel square lattices in the ab -plane separated along the c -axis by LaO layers, resulting in the compound’s quasi 2D nature. The lattice parameters were found to be $a = 4.1027$ Å and $c = 9.0781$ Å, consistent with the previously reported values $a = 4.10492$ Å and $c = 9.08178$ Å [17], and within 5% of the LaFeAsO lattice parameters $a = 4.0355$ Å and $c = 8.7393$ Å [15]. The lattice parameters monotonically increase with Ba and Mn doping up to $x = 0.15$, indicating the successful solid solution of (La,Ba) and (Zn,Mn). Impurity phases of La_2O_3 and ZnAs_2 start to appear at $x = 0.1$ and grows prominently through $x = 0.20$, as marked by the arrows and stars in Fig. 1(a).

In Fig. 2(b), we show the zero-field cooled (ZFC) and field cooled (FC) measurements of the dc -magnetization M for $B_{ext} = 1000$ Oe. A significant increase in M is observed at temperatures of $30\text{ K} \sim 40\text{ K}$, and the ZFC and FC curves split at low temperatures for all doping levels. Interestingly, we do not observe such features in Mn-doped LaZnAsO, $\text{LaZn}_{0.9}\text{Mn}_{0.9}\text{AsO}$, as shown by the magnetization curve in Fig. 2(a). Instead, $\text{LaZn}_{0.9}\text{Mn}_{0.9}\text{AsO}$ remains paramagnetic down to 2 K, where M is about an order of magnitude smaller than for $(\text{La}_{0.9}\text{Ba}_{0.1})(\text{Zn}_{0.9}\text{Mn}_{0.1})\text{AsO}$. This indicates that although doping Mn introduces local moments, the ferromagnetic ordering will not develop unless the spins are mediated by carriers arising from (La,Ba) substitutions. This picture is similar to the case of $(\text{Ga},\text{Mn})\text{As}$ system where Zener’s model [18] is proposed as one candidate to explain the ferromagnetism. In this theoretical model, RKKY-like interaction of Mn spins are effectively mediated by hole carriers in the valence band.

The saturation moment has a maximum of $0.95 \mu_B/\text{Mn}$ for $x = 0.05$ and decreases monotonically with increasing x , falling to a value of $0.17 \mu_B/\text{Mn}$ for $x = 0.20$. This likely results from competition between the RKKY interaction, whose first oscillation period supports ferromagnetic coupling, and nearest neighbor (NN) antiferromagnetic coupling via direct exchange interaction. For $x = 0.1$, the probability of finding two Mn atoms at NN Zn sites is $P(N;x) = C_N^4 \cdot x^N \cdot (1-x)^N = 29.16\%$, where $N = 1$ and $x = 0.1$. The direct antiferromagnetic coupling between the Mn-Mn pairs causes antiferromagnetic ordering in LaMnAsO at $T_N = 317\text{ K}$ [19].

We fit the temperature dependence of M above T_C to a Curie-Weiss law. The effective paramagnetic moment is about $4 - 5 \mu_B/\text{Mn}$, as expected for fully magnetic individual Mn^{2+} moments. The isothermal magnetization of $(\text{La}_{1-x}\text{Ba}_x)(\text{Zn}_{1-x}\text{Mn}_x)\text{AsO}$ at 5 K is plotted in Fig. 2(c). The parallelogram-shaped hysteresis loops show coercive fields of 1.06, 1.14, 1.28 and 0.71 T for $x = 0.05$,

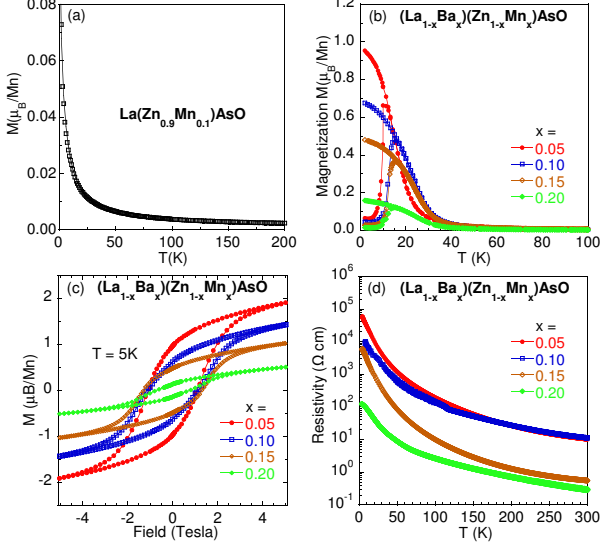


FIG. 2: (Color online) (a) The magnetization M for $\text{LaZn}_{0.9}\text{Mn}_{0.1}\text{AsO}$, without charge doping; the solid line represents the Curie-Weiss law. (b)-(d): Results on $(\text{La}_{1-x}\text{Ba}_x)(\text{Zn}_{1-x}\text{Mn}_x)\text{AsO}$: (b) M obtained in the zero field cooling (ZFC) and field cooling (FC) in the external field of 1000 Oe. (c) The isothermal magnetization measured at 5 K. (d) The electrical resistivity.

0.10, 0.15 and 0.20, respectively, much larger than the ~ 50 Oe coercive field in the cubic $\text{Li}_{1.1}(\text{Zn}_{0.97}\text{Mn}_{0.03})\text{As}$ [9] and $(\text{Ga}_{0.965}\text{Mn}_{0.035})\text{As}$ [1]. The large coercive field is also reflected in the large differences between the ZFC and FC curves at low temperature (Fig. 2(b)). The 2D crystal structure of $(\text{La}_{1-x}\text{Ba}_x)(\text{Zn}_{1-x}\text{Mn}_x)\text{AsO}$ may cause the large coercive field, as a similar situation was found in $(\text{Ba},\text{K})(\text{Zn},\text{Mn})_2\text{As}_2$, another 2D DMS system [13]. Efforts are currently underway to generate single crystals to further investigate the anisotropic properties within the ab -plane and along the c -axis.

In Fig. 2(d), we show electrical resistivity measurements for $(\text{La}_{1-x}\text{Ba}_x)(\text{Zn}_{1-x}\text{Mn}_x)\text{AsO}$. All samples display typical semiconducting behavior over the entire temperature range. The resistivity decreases as more carriers are introduced through higher charge doping levels. For $x = 0.05$, the resistivity is on the order of $10^4 \Omega\text{ cm}$, two orders of magnitude larger than that of $\text{Li}(\text{Zn},\text{Mn})\text{As}$ [9]. This large resistivity precluded Hall effect measurements on these polycrystalline specimens. In recent papers [20, 21], Liu et al. observed Kondo-like behavior in Mn-doped CaNiGe and CaNiGeH , where the resistivity decreases linearly with decreasing temperature down to 20 K and then increases upon further cooling. This is in contrast to the behavior observed in our compounds.

The availability of bulk specimens enabled us to perform conventional μSR experiments on $(\text{La}_{1-x}\text{Ba}_x)(\text{Zn}_{1-x}\text{Mn}_x)\text{AsO}$. To determine the nature of the magnetic order, we conducted zero field (ZF), longitudinal field (LF), and weak transverse field

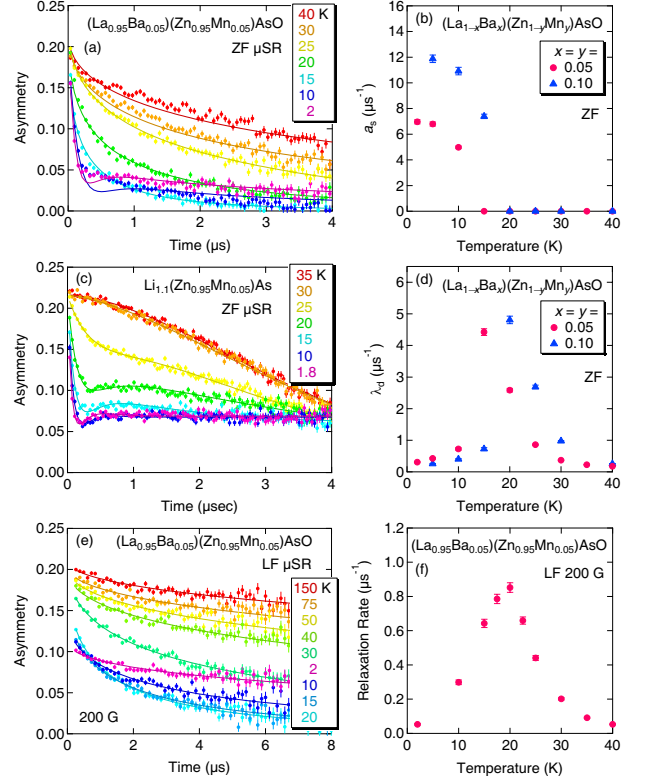


FIG. 3: (Color online) Zero field μSR time spectra of (a) $(\text{La}_{0.95}\text{Ba}_{0.05})(\text{Zn}_{0.95}\text{Mn}_{0.05})\text{AsO}$ (present work) and (c) $\text{Li}_{1.1}(\text{Zn}_{0.95}\text{Mn}_{0.05})\text{As}$ (adapted from ref. [9]). The solid lines in (a) show a fit to a dynamic-static relaxation function (eq. 24 of ref. [22]) with the static local field amplitude parameter a_s shown in (b) and the dynamic relaxation rate parameter λ_d in (d). The solid lines in (c) represent a fit to the “volume fraction model” described in ref. [9]. (b) and (d) also include the results for $(\text{La}_{0.9}\text{Ba}_{0.1})(\text{Zn}_{0.9}\text{Mn}_{0.1})\text{AsO}$. Figure (e) shows the time spectra of LF- μSR in $(\text{La}_{0.95}\text{Ba}_{0.05})(\text{Zn}_{0.95}\text{Mn}_{0.05})\text{AsO}$ with a longitudinal field of 200 G and (f) shows the muon spin relaxation rate $1/T_1$ due to dynamic spin fluctuations.

(WTF) μSR measurements for $x = 0.05$ and ZF and WTF measurements for $x = 0.1$. Fig. 3(a) displays the time spectra of ZF- μSR for $x = 0.05$, showing a rapid increase of muon spin relaxation for temperatures below $T \sim 30$ K. Several interesting differences are observed between the current results and the ZF- μSR time spectra from the cubic $\text{Li}_{1.1}(\text{Zn}_{0.95}\text{Mn}_{0.05})\text{As}$, as illustrated in Fig. 3(c) (adapted from Fig. 3(a) of ref. [9]). The spectra for the “111” system in Fig. 3(c) are well described by the sum of a static relaxation function representing the magnetically ordered volume and an exponentially decaying dynamic relaxation function representing the remaining volume in the paramagnetic phase. The time spectra of the present “1111” system exhibit characteristic signatures of dynamic slowing down followed by static magnetic order, behavior also observed in spin glasses AuFe and CuMn [22]. Despite the imperfections of the fit, evidenced by the differences

between the data and the fit curves in Fig. 3(a), we plot in Figs. 3(b) and (d) the refined static random field amplitude a_s and dynamic relaxation rate λ_d found in the relaxation function given in eq. 24 of ref. [22].

To further study the dynamic spin fluctuations, we performed LF- μ SR measurements on the “1111” DMS system with $x = 0.05$ in LF = 200 G. Analysis of the time spectra displayed in Fig. 3(e) yields the LF relaxation rate $1/T_1$ shown in Fig. 3(f), which exhibits a clear peak at $T \sim 15 - 20$ K, consistent with the peak temperature of λ_d in ZF (Fig. 3(d)) and the onset temperature of the static spin freezing represented by a_s (Fig. 3(b)). ZF- μ SR results for $x = 0.1$ yield similar results for a_s and λ_d , as shown in Figs. 3(b) and (d). LF- μ SR measurements were not performed on the $x = 0.1$ system due to beamtime constraints. We note that for both $x = 0.05$ and $x = 0.1$, the onset temperature of a_s in ZF and the “spin freezing” temperature indicated by the peaks of λ_d in ZF and $1/T_1$ in LF agree well with the temperature below which the FC and ZFC magnetization in Fig. 2(b) show a remarkable departure.

In general, the history dependent behavior can be found both in many regular ferromagnets due to formation and motion of magnetic domains [23], and in spin glasses due to multiple minima of free energy as a function of spin configurations [24]. In some cases z-component of the spin behaves as ferromagnets while x- and y-components as spin glasses [24, 25]. Detailed distinction of these three different cases requires not only the magnetization data but also neutron scattering results for spatial spin correlations. Since magnetic neutron scattering signal cannot be observed due to spatially dilute Mn moments and lack of single crystal specimens, there is no definite evidence at this moment to allow distinguishing between ferromagnetic and spin glass states for the present system.

Practically speaking, however, there is a clear difference between typical ferromagnets and spin glasses in their magnitudes of the saturation moment size in the ground state at low temperatures obtained in zero field after training in high external magnetic fields. In many ferromagnets, the remnant magnetization value is in the order of Bohr magneton per magnetic atom, while in typical dilute alloy spin glasses, it is 0.01 Bohr magneton per magnetic atom or less [26–28]. In the present system, this remanent magnetization is approximately 1 Bohr magneton per Mn, as shown in Fig. 2(c). Therefore, we tentatively assign the present system to a ferromagnet, rather than to a spin glass.

Use of the so-called “spin glass relaxation function” [22] to fit the μ SR data does not provide any distinction between ferromagnetic and spin glass systems, especially for the cases with spatially dilute magnetic moments. For example, the earlier μ SR results on well established ferromagnets (Ga,Mn)As fitted quite well to the spin glass relaxation function [8].

Analyzed with either the “volume fraction” fitting used in the “1111” DMS [9], “122” DMS [13], and (Ga,Mn)As

[8] systems or the “dynamic spin freezing” model used in the present “1111” system, ZF- μ SR results indicate that these systems all achieve static magnetic order throughout nearly the entire volume at low temperatures. A closely linear relationship between the local field amplitude parameter a_s and the Curie temperature T_C was first noticed in (Ga,Mn)As (Fig. 3(d) of ref. [8]) and Li(Zn,Mn)As (Fig. 3(d) of ref. [9]). In Fig. 4, we plot a_s versus T_C for the two former systems, the “122” system (Ba,K)(Zn,Mn)₂As₂ [13], and the present (La,Ba)(Zn,Mn)AsO system. The universal linear trend suggests that the exchange interaction supporting ferromagnetic coupling in these systems has a common origin and comparable magnitude for a given spatial density of ordered moments.

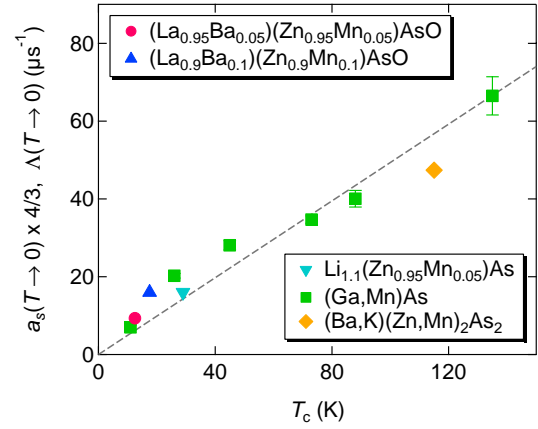


FIG. 4: (Color online) Correlation between the static internal field parameter a_s determined at $T = 2$ K by zero-field μ SR versus the ferromagnetic Curie temperature T_C observed in (Ga,Mn)As [8], Li(Zn,Mn)As [9], (La,Ba)(Zn,Mn)AsO (the present work) and (Ba,K)(Zn,Mn)₂As₂ [13]. Nearly linear correlation indicates a common mechanism for the ferromagnetic exchange interaction.

Magnetization, transport, and μ SR studies carried out in (Ga_{1-x}Mn_x)As [8] demonstrated that ferromagnetic order is achieved for small Mn concentrations ($x = 0.012 - 0.030$) even before the system undergoes the semiconductor to metal transitions. In other words, hole carriers that are not fully delocalized can mediate the ferromagnetic exchange interaction with magnitude comparable to those in the case of full delocalization. It is interesting to note that the quasi 2D “1111” (present work) and “122” [13] DMS systems both exhibit ferromagnetism with relatively high T_C while the charge carriers still remain semiconducting. The average size of ordered Mn moments in the “1111” and “122” systems is significantly smaller than in (Ga,Mn)As with T_C above ~ 40 K. This feature suggests that some of the Mn moments are not involved in the percolating ferromagnetic network in the semiconducting DMS systems. The difference between the cubic systems (Ga,Mn)As and Li(Zn,Mn)As and the 2D DMS systems may also indicate that metallic conduction is eas-

ier to achieve in 3D systems due to a lower percolation threshold.

In summary, we reported the synthesis of the “1111” DMS ferromagnet $(\text{La}_{1-x}\text{Ba}_x)(\text{Zn}_{1-x}\text{Mn}_x)\text{AsO}$, as the third DMS family which has a direct counterpart among the FeAs superconductor families. As discussed in earlier papers [9, 13], the common crystal structure and excellent lattice matching open doors to the future development of junction devices based on the companion ferromagnetic and superconducting materials. In parallel with the present study, the IOP-Beijing group among the present authors has synthesized another “1111” DMS ferromagnet, $(\text{La,Ba})(\text{Zn,Mn})\text{SbO}$, which will be reported separately [29].

The work at Zhejiang University was supported by National Basic Research Program of China (No. 2011CBA00103), NSFC(No.11274268), Zhejiang Provincial NSFC(LY12A04006) and Fundamental Research Funds for Central Universities (2013QNA3016); at IOP in Beijing by the NSFC and MOST; at Columbia by the US NSF PIRE (Partnership for International Research and Education: OISE-0968226) and DMR-1105961 projects; the JAEA Reimei project at IOP, Columbia, PSI, McMaster; and NSERC and CIFAR at McMaster. We would like to thank C. Cao, A. Fujimori, B. Gu, S. Maekawa and H. Suzuki for helpful discussions.

-
- [1] H. Ohno, A. Shen, F. Matsukura, A. Oiwa, A. Endo, S. Katsumoto, and Y. Iye, *Appl. Phys. Lett.* **69**, 363 (1996).
 - [2] T. Jungwirth, J. Sinova, J. Masek, J. Kucera, and A.H. MacDonald, *Rev. Mod. Phys.* **78**, 809 (2006).
 - [3] T. Dietl, *Nature Materials* **9**, 965 (2010).
 - [4] I. Zutic, J. Fabian, and S. Das Sarma, *Rev. Mod. Phys.* **76**, 323 (2004).
 - [5] M. Wang, R.P. Campion, A.W. Rushforth, K.W. Edmonds, C.T. Foxon, and B.L. Gallagher, *Appl. Phys. Lett.* **93**, 132103 (2008).
 - [6] N. Samarth, *Nature Materials* **9**, 955 (2010).
 - [7] S. Chambers, *Nature Materials* **9**, 956 (2010).
 - [8] S.R. Dunsiger, J.P. Carlo, T. Goko, G. Nieuwenhuys, T. Prokscha, A. Suter, E. Morenzoni, D. Chiba, Y. Nishitani, T. Tanikawa, F. Matsukura, H. Ohno, J. Ohe, S. Maekawa, and Y.J. Uemura, *Nature Materials* **9**, 299 (2010).
 - [9] Z. Deng, C.Q. Jin, Q.Q. Liu, X.C. Wang, J.L. Zhu, S.M. Feng, L.C. Chen, R.C. Yu, C. Arguello, T. Goko, F.L. Ning, J.S. Zhang, Y.Y. Wang, A.A. Aczel, T. Munzie, T.J. Williams, G.M. Luke, T. Kakeshita, S. Uchida, W. Higemoto, T.U. Ito, B. Gu, S. Maekawa, G.D. Morris, and Y.J. Uemura, *Nature Communications* **2**, 422 (2011).
 - [10] J. Masek, J. Kudrnovsky, F. Maca, B.L. Gallagher, R.P. Campion, D.H. Gregory, and T. Jungwirth, *Phys. Rev. Lett.* **98**, 067202 (2007).
 - [11] X.C. Wang, Q.Q. Liu, Y.Y. Lv, W.B. Gao, S.M. Feng, L.X. Yang, R.C. Yu, F.Y. Li, and C.Q. Jin, *Solid State Communications* **148**, 538 (2008).
 - [12] D.R. Parker, M.J. Pitcher, P.J. Baker, I. Franke, T. Lancaster, S.J. Blundell, and S.J. Clarke, *Chemical Communications*, 2189 (2009).
 - [13] K. Zhao, Z. Deng, X.C. Wang, W. Han, J.L. Zhu, X. Li, Q.Q. Liu, T. Goko, B. Frandsen, L. Liu, F.L. Ning, Y.J. Uemura, H. Dabkowska, G.M. Luke, H. Leutkens, E. Morenzoni, S.R. Dunsiger, A. Senyshyn, P. Boeni, and C.Q. Jin, *Nature Communications* **4**, 1422 (2013).
 - [14] D.C. Johnston, *Adv. Phys.* **59**, 803 (2010).
 - [15] Y. Kamihara, T. Watanabe, M. Hirano, and H. Hosono, *J. Am. Chem. Soc.* **130**, 3296 (2008).
 - [16] K. Kayanuma, R. Kawamura, H. Hiramatsu, H. Yanagi, M. Hirano, T. Kamiya, and H. Hosono, *Thin Solid Films* **516**, 5800 (2008).
 - [17] Y. Takano, S. Komaatsuzaki, H. Komasaki, T. Watanabe, Y. Takahashi, and K. Takase, *J. Alloys. Compd.* **451**, 467 (2008).
 - [18] T. Dietl, H. Ohno, F. Matsukura, J. Cibert, and D. Ferrand, *Science* **287**, 1019 (2000).
 - [19] N. Emery, E.J. Wildman, J.M.S. Skakle, A.C. McLaughlin, R.I. Smith, and A.N. Fitch, *Phys. Rev. B* **83**, 144429 (2011).
 - [20] X.F. Liu, S. Matsuishi, S. Fujitsu, and H. Hosono, *Phys. Rev. B* **84**, 214439 (2011).
 - [21] X.F. Liu, S. Matsuishi, S. Fujitsu, T. Ishigaki, T. Kamiyama, and H. Hosono, *J. Am. Chem. Soc.* **134**, 11687 (2012).
 - [22] Y.J. Uemura, T. Yamazaki, D.R. Harshman, M. Senba, and E.J. Ansaldo, *Phys. Rev. B* **31**, 546 (1985).
 - [23] N.W. Ashcroft, and N.D. Mermin, *Solid State Physics* (Holt, Rinehart and Winston, 1976).
 - [24] K.H. Fischer, and J.A. Hertz, *Spin Glasses* (Cambridge University Press, 1991).
 - [25] I. Mirebeau, P41, *Recent Progress in Random Magnets* (Edited by D.H. Ryan, World Scientific Publishing Co. Pte. Ltd, 1992).
 - [26] J.L. Tholence, and R. Tournier, *J. Phys. (Paris)* **35**, C4-229 (1974).
 - [27] J.J. Prejean, M. Joliclerc, and P. Monod, *J. Phys. (Paris)* **41**, 427 (1980).
 - [28] P. Monod, J.J. Prejean, and B. Tissier, *J. Appl. Physics* **50**, 7324 (1979).
 - [29] W. Han, F.L. Ning, Y.J. Uemura, and C.Q. Jin, to be submitted.